IEEE Photonics Journal
An IEEE Photonics Society Publication

Nonuniformity Correction for Variable-Integration-Time Infrared Camera

Volume 10, Number 6, December 2018

Nan Chen, *Member, IEEE*
Jiqing Zhang
Shengyou Zhong
Zhongshun Ji
Libin Yao, *Senior Member, IEEE*

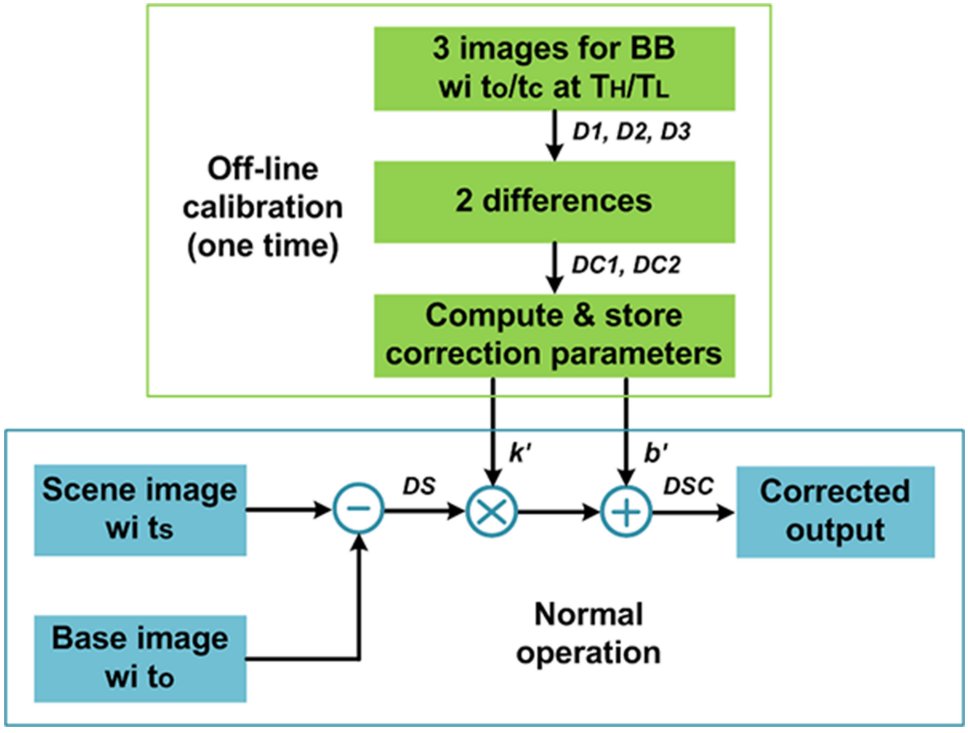

DOI: 10.1109/JPHOT.2018.2881393
1943-0655 © 2018 IEEE

Nonuniformity Correction for Variable-Integration-Time Infrared Camera

Nan Chen, *Member, IEEE*, Jiqing Zhang, Shengyou Zhong, Zhongshun Ji, and Libin Yao, *Senior Member, IEEE*

Kunming Institute of Physics, Kunming 650223, China

DOI:10.1109/JPHOT.2018.2881393

Manuscript received September 25, 2017; revised June 2, 2018; accepted November 10, 2018. Date of publication November 15, 2018; date of current version November 29, 2018. This work was supported in part by the Applied Basic Research Programs of Yunnan Province under Grant 2013FC009.
Corresponding author: Libin Yao (e-mail: libinyao@ieee.org).

Abstract: A two-dimensional calibration technique is proposed to correct the spatial nonuniformity in infrared imaging systems adapting to different integration time and time-varying offset with one-time calibration. Differing from traditional calibration-based nonuniformity correction, this method calibrates nonuniformity with two-dimensional information from two integration time besides different irradiance, which conquers drawbacks of traditional calibration-based correction. First, it eliminates the dependence on integration time in calibration process and dramatically suppresses fixed pattern noise by a large attenuation factor. In addition, time-varying offset is real-time canceled by the subtraction of images integrated with normal and short time. Correction error of two-point correction and the proposed method are analyzed in detail. In experiments with cooled infrared camera, the proposed method provides enhanced uniformity even for seven-time variation of integration time using same correction coefficients. Both quantitative and qualitative comparisons to two-point correction demonstrate its superiority. The one-time calibration and shutterless correction scheme avoids interruption of the normal operation for real scene, extending the application range in practical engineering for infrared imaging systems with low complexity of computation and hardware.

Index Terms: Infrared imaging, nonuniformity correction.

1. Introduction

Spatial nonuniformity severely degrades the image quality of infrared camera, which is mainly caused by the response deviation of detectors in focal plane array (FPA), mismatch of readout electronics, and other components in imaging system [1]. The nonuniformity, also known as fixed patter noise (FPN), is usually reduced by nonuniformity correction (NUC) implemented by hardware or software, including calibration-based NUC and scene-based NUC.

Two-point correction (TPC) [2] has been widely used in practical engineering application due to its low computation complexity and easy implementation of hardware. TPC is based on the assumption of linear response to target temperature, while its correction error increases for wide dynamic range since the response is nonlinear in a wider temperature range [3], [4]. To solve this problem, piecewise linear method [5] divides the operation range into multiple sections, and uses TPC for each section. This requires to store multiple groups of correction coefficients, and the appropriate section needs to be selected for a particular pixel output by additional control logic. Multi-point correction is proposed to deal with these drawbacks, which uses first-order [6],

second-order polynomial [7] or least-square curve fitting [8] to extend the operation range with one group of coefficients. Correction based on S-curve model is also proposed to resolve the problem of nonlinear response [9], [10].

The second issue of calibration-based correction is the offset drift with operating time and condition, including variation of FPA temperature and bias voltage, thereby degrades correction performance. Additional uniform target, such as shutter, can be used to correct the time-varying offset accompanied by TPC [11]. Although the additional one-point correction eliminates the offset FPN, it disturbs the camera's normal operation for real scene. To achieve real-time correction, an online offset estimation scheme is proposed in [12], which relies on prior knowledge of the offset dependence on the FPA temperature to calculate the offset coefficients to compensate the temperature drift. As the validity of this algorithm is determined by the accuracy of FPA temperature measurements, its correction performance is not as good as one-point correction.

In addition, the residue nonuniformity of calibration-based correction is proportional to the difference between integration time in normal operation and off-line calibration [2]. Therefore, integration time is limited to a particular one for best correction performance, otherwise re-calibration is required with interruption of normal operation for other integration time. Alternatively, multiple groups of correction coefficients for different integration time should be computed and stored. The fixed integration time limits the application range for different scene requiring variable integration time.

Therefore, more research works focus on scene-based correction for adaptive correction [13]–[19]. Since the correction is performed with images of real scene, it shows better correction performance for time-varying offset and variable integration time. However, its complex algorithm prevents the implementation of hardware and real-time processing, thus most scene-based correction methods are studied in laboratory. Ghosting artifacts is another limitation for practical application of these methods [16]. An algebraic scene-based algorithm is proposed in [19] for bias nonuniformity correction, which is computationally efficient and easily implemented compared to other scene-based algorithms. But its correction effect is strongly dependent on the accuracy of estimated shift.

In this paper, a shutter-less two-dimensional calibration scheme is proposed to correct spatial nonuniformity of infrared image for variable integration time and time-varying offset. This method calibrates nonuniformity with two-dimensional information from both temperature and integration time to suppress FPN for arbitrary integration time, and eliminates time-varying offset by the cancellation with base image. The proposed calibration-based NUC features real-time processing because of its simple algorithm and low requirement of hardware. The experimental results with cooled infrared camera verified the effectiveness of the proposed scheme compared to traditional two-point NUC.

The remainder of this paper is organized as follows. In Section 2, based on the proposed model, correction error of traditional TPC is theoretically analyzed. The proposed scheme is presented and analyzed in detail in Section 3. Section 4 shows the experiments and discussion, followed by the conclusions in Section 5.

2. Two-Point Correction

2.1 Analysis Model

For better understanding of nonuniformity, the response model of infrared imaging system should be considered. According to [2], the gray level of pixel (i, j) can be represented by its gray level as

$$D_{i,j}(t, T) = tG_{i,j}L(T) + O_{i,j} \tag{1}$$

where t is the integration time, and T is the temperature of target. $G_{i,j}$ is the gain of pixel (i, j) from its radiance to the gray level expressed as

$$G_{i,j} = \tau_{eff} S_{i,j} \Omega_{i,j} K_{i,j} \tag{2}$$

in which $\tau_{i,j}$ is the effective transmittance of optical system, $S_{i,j}$ is the active area, $\Omega_{i,j}$ is the projected solid angle, and $K_{i,j}$ is the gain of analog-to-digital converter.

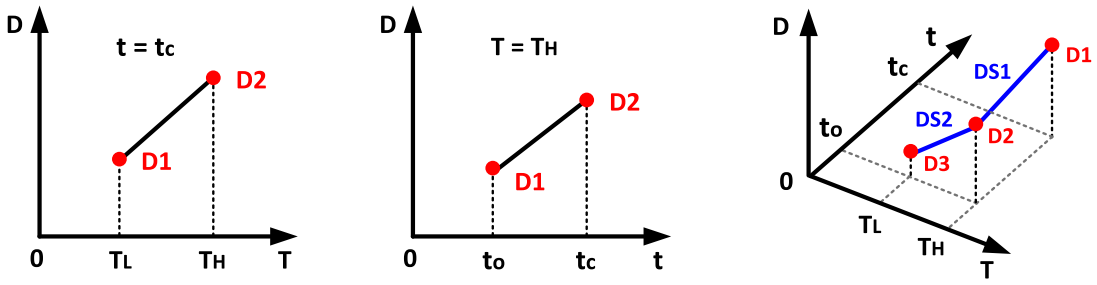

Fig. 1. Calibration data for (a) different temperature, (b) different integration time and (c) the proposed two-dimensional calibration.

The radiance at temperature T is

$$L(T) = \int_{\lambda 1}^{\lambda 2} L(\lambda, T)\, \eta(\lambda) d\lambda \tag{3}$$

where $L(\lambda, T)$ and $\eta(\lambda)$ are the spectral radiance at temperature T for wavelength of λ and corresponding quantum efficiency, respectively. $\lambda 1$ and $\lambda 2$ are the upper and lower cutoff wavelength.

The dispersion of $G_{i,j}$ and $L(\lambda, T)$ give rise to the gain FPN, and $O_{i,j}$ contributes to the offset FPN. Above model simply treats all offset as a fixed component and ignores the fact that the gray level arising from dark current is associated with integration time. In addition, offset is time-varying in practice because the FPA temperature and bias voltage will drift with operation time.

A improved model is presented to feature these effects more adequately as

$$D_{i,j}^{V}(t, T) = t[G_{i,j} L(T) + B_{i,j}] + [V A_{i,j} + O_{i,j}] \tag{4}$$

In this model, nonuniformity of dark current contributes to the gain FPN associated with integration time by factor $B_{i,j}$. In addition to the fixed offset $O_{i,j}$, time-varying offset is also considered by bias voltage V and its gain of $A_{i,j}$. Temperature variation of FPA can be ignored as it works with a temperature stabilization by cooler.

2.2 Two-Point Correction

As shown in Fig. 1(a), calibration images of TPC are captured for blackbody at two reference temperatures (T_H, T_L) with integration time of t_C, thus they only contain one-dimensional information of temperature. The corresponding digital codes of pixel (i, j) are shown as follows, respectively.

$$D1 = D_{i,j}^{V_C}(t_C, T_L) = t_C[G_{i,j} L(T_L) + B_{i,j}] + (V_C A_{i,j} + O_{i,j}) \tag{5}$$

$$D2 = D_{i,j}^{V_C}(t_C, T_H) = t_C[G_{i,j} L(T_H) + B_{i,j}] + (V_C A_{i,j} + O_{i,j}) \tag{6}$$

where V_C is the bias voltage in the calibration process.

The gain and offset correction coefficients of pixel (i, j) are calculated by following equations, respectively [2].

$$k_{i,j} = \frac{\overline{D1} - \overline{D2}}{D1_{i,j} - D2_{i,j}} \tag{7}$$

$$b_{i,j} = \overline{D1} - k_{i,j} D1_{i,j} \tag{8}$$

where $\overline{D1}$ and $\overline{D2}$ are spatial mean output codes of all pixels at temperature of T_H and T_L, respectively. For a FPA with M columns and N rows, its mean output code at temperature of T, with

integration time of t, and with bias voltage of V is given by

$$\overline{D^V(t,T)} = \frac{1}{MN}\sum_{i=1}^{M}\sum_{j=1}^{N} D_{i,j}^{V}(t,T) = t\left[\overline{G}L(T) + \overline{B}\right] + \left(V\overline{A} + \overline{O}\right) \tag{9}$$

where $\overline{G}$, $\overline{A}$, $\overline{B}$ and $\overline{O}$ are the corresponding spatial mean value of each variable, respectively.

In normal operation, the output code for real scene with temperature of T after integration time of t_S is

$$D_{i,j}^{V_S}(t_S,T) = t_S[G_{i,j}L(T) + B_{i,j}] + (V_S A_{i,j} + O_{i,j}) \tag{10}$$

where V_S is the bias voltage in normal operation. The final output code after TPC is computed by [2]

$$DC_{i,j}^{V_S}(t_S,T) = k_{i,j}D_{i,j}^{V_S}(t_S,T) + b_{i,j} \tag{11}$$

The correction error of pixel (i, j) can be evaluated by the difference between its corrected code and the mean code of FPA as

$$\Delta_{i,j} = DC_{i,j}^{V_S}(t_S,T) - \overline{D^{V_S}(t_S,T)} = \frac{(t_S - t_C)(\overline{G}B_{i,j} - \overline{B}G_{i,j})}{G_{i,j}} + (V_S - V_C)\left(A_{i,j}\frac{\overline{G}}{G_{i,j}} - \overline{A}\right) \tag{12}$$

Obviously, gain FPN can be cancelled when integration time in normal operation and calibration are same ($t_S = t_C$), thus the infrared image has to be captured with a particular integration time for the best correction performance. Whereas offset FPN would not be eliminated if there are difference between bias voltage in normal operation and calibration, which is always true in practice due to that supply voltage and bias will drift with operation time. Consequently, dependence on integration time and time-varying offset limit the correction performance of TPC [2], as well as other calibration-based correction schemes [3]–[10].

3. Two-Dimensional Calibration

Limitation of integration time in TPC comes from the truth that its calibration images only contain information of different reference temperatures. To solve this problem, we can explore more information for calibration. According to the response model in (4), the output code and integration time exhibit linear relation, as shown in Fig. 1(b). Thus if we add information of different integration times into calibration images, the calibration will be two-dimensional. Illustrated in Fig. 1(c), three images against blackbody at two temperatures (T_H, T_L) and integrated with two different periods (t_C, t_0) are captured as follows, respectively.

$$D1_{i,j} = D_{i,j}^{V_C}(t_C,T_H) = t_C[G_{i,j}L(T_H) + B_{i,j}] + (V_C A_{i,j} + O_{i,j}) \tag{13}$$

$$D2_{i,j} = D_{i,j}^{V_C}(t_0,T_H) = t_0[G_{i,j}L(T_H) + B_{i,j}] + (V_C A_{i,j} + O_{i,j}) \tag{14}$$

$$D3_{i,j} = D_{i,j}^{V_C}(t_0,T_L) = t_0[G_{i,j}L(T_L) + B_{i,j}] + (V_C A_{i,j} + O_{i,j}) \tag{15}$$

in which we set that $t_0 << t_C$.

Then we use the difference of these images as calibration images to combine information of temperature and integration time.

$$DC1_{i,j} = D1_{i,j} - D2_{i,j} = (t_C - t_0)[G_{i,j}L(T_H) + B_{i,j}] \tag{16}$$

$$DC2_{i,j} = D2_{i,j} - D3_{i,j} = t_0 G_{i,j}[L(T_H) - L(T_L)] \tag{17}$$

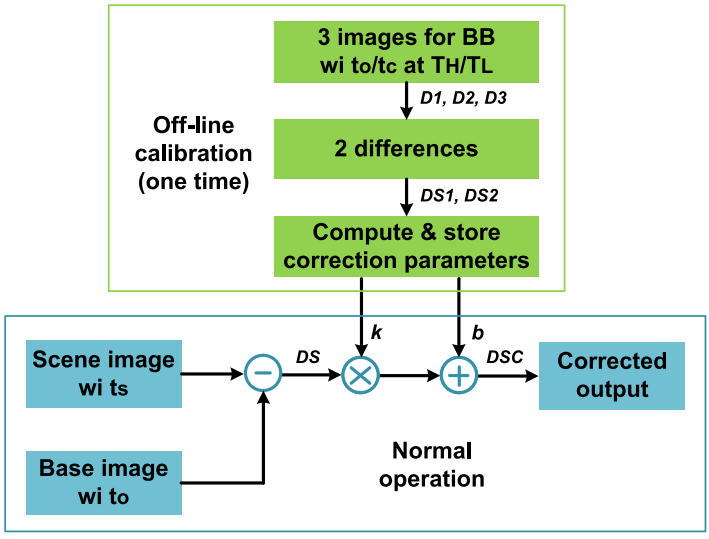

Fig. 2. Flowchart of the proposed two-dimensional NUC.

The gain and offset correction coefficients are obtained by *DC1* and *DC2* as follows.

$$k'_{i,j} = \frac{\overline{DC1} - \overline{DC2}}{DC2_{i,j} - DC2_{i,j}} \tag{18}$$

$$b'_{i,j} = \overline{DC1} - k'_{i,j} DC1_{i,j} \tag{19}$$

In normal operation for real scene, a base image is captured firstly with small integration time of t_0, then the image integrated with time of t_S ($t_S >> t_0$) is captured. The drift of bias voltage can be neglected since the time interval between the two images is very short.

$$D_{i,j}^{V_S}(t_0, T) = t_0[G_{i,j}L(T) + B_{i,j}] + [V_S A_{i,j} + O_{i,j}] \tag{20}$$

$$D_{i,j}^{V_S}(t_S, T) = t_S[G_{i,j}L(T) + B_{i,j}] + [V_S A_{i,j} + O_{i,j}] \tag{21}$$

The two images are subtracted to cancel the offset including components correlating with bias voltage.

$$DS_{i,j}(t_S, T) = D_{i,j}^{V_S}(t_S, T) - D_{i,j}^{V_S}(t_0, T) = (t_S - t_0)[G_{i,j}L(T) + B_{i,j}] \tag{22}$$

Obviously all offsets are totally eliminated by the subtraction even without additional NUC.
The difference from (22) is corrected by parameters from (18) and (19) as

$$DSC_{i,j}(t_S, T) = k'_{i,j} DS_{i,j}(t_S, T) + b'_{i,j} \tag{23}$$

The operation flow of the proposed two-dimensional calibration and correction method is shown in Fig. 2, in which the calibration only performs once, and the computed correction coefficients are used in normal operation for variable integration time avoiding interruption by shutter. The computation complexity of the presented method is as low as traditional two-point correction.
The correction error of the proposed method can be derived as

$$\Delta'_{i,j} = DSC_{i,j}(t_S, T) - \overline{DS(t_S, T)} \approx t_S(\overline{G}B_{i,j} - \overline{B}G_{i,j})\frac{L(T) - L(T_L)}{G_{i,j}L(T_H) + B_{i,j}}$$

$$= t_S(\overline{G}B_{i,j} - \overline{B}G_{i,j})\alpha \tag{24}$$

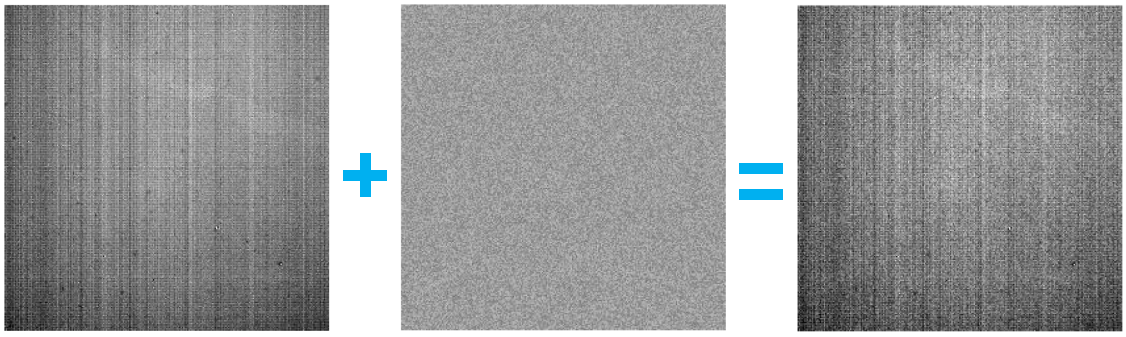

Fig. 3. Images for the first experiment: (a) captured raw scene image, (b) random offset (FPN = 0.5%), and (c) image with additional random offset.

where α is the attenuation factor expressed as

$$\alpha = \frac{L(T) - L(T_L)}{G_{i,j}L(T_H) + B_{i,j}} = \frac{L(T) - L(T_L)}{D^0_{i,j}(1, T_H)} \tag{25}$$

where $D^0_{i,j}(1, T_H)$ is the gray level of calibration image at high temperature (T_H) after 1-second integration without offset. This factor will effectively suppress the correction error since $D^0_{i,j}(1, T_H)$ is very large.

Compared to two-point correction, the proposed method not only cancels offset FPN, but also eliminates the dependence on integration time in calibration process (t_C). By the help of attenuation factor, it is expected that FPN with the proposed technique will be suppressed to a low level even with different integration time in normal operation.

4. Experimental Results

A 256 × 256 cooled mid-wave infrared (MWIR) camera is used to test the proposed scheme compared to two-point correction. The prototype camera contains a custom-designed readout circuit with column-parallel ADCs and integration time controller, as well as FPGA-based image processing circuits.

The calibration images are captured for black body at temperature of 20 °C (T_L) and 40 °C (T_H), with integration time of 16 μs (t_0) and 1.5 ms (t_C). Correction coefficients of TPC are calculated by (5)–(9), and the proposed NUC are implemented by (13)–(19). These correction coefficients are used for the following experiments.

The spatial nonuniformity is evaluated by FPN, defined as the spatial standard deviation over the maximum non-saturated gray level as

$$FPN = \frac{1}{D_{\max}} \sqrt{\frac{1}{MN} \sum_{i=1}^{M} \sum_{j=1}^{N} \left[D_{i,j}(t_S, T) - \overline{D(t_S, T)} \right]^2} \tag{26}$$

where $M = N = 256$ in the tested camera, and the maximum gray level is 14450.

Spatial signal-to-noise ratio (SNR) is also defined to evaluate the performance as

$$SNR = 20 \log \frac{\overline{D(t_S, T)}}{\sqrt{\frac{1}{MN} \sum_{i=1}^{M} \sum_{j=1}^{N} \left[D_{i,j}(t_S, T) - \overline{D(t_S, T)} \right]^2}} \tag{27}$$

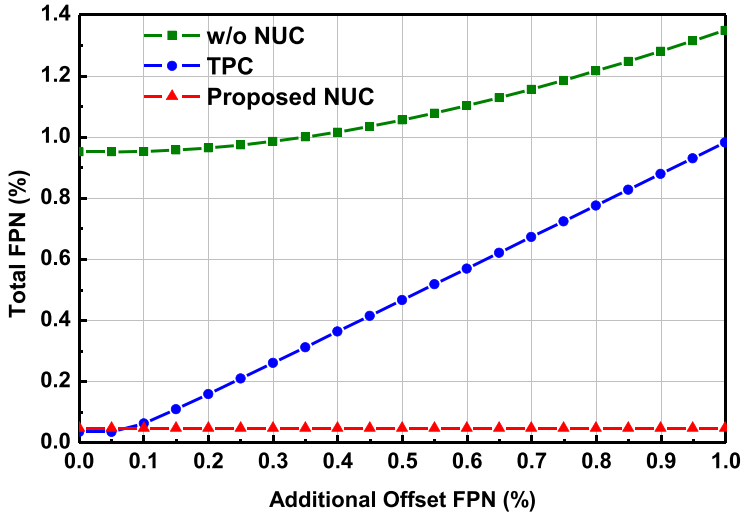

Fig. 4. Measured FPN of raw image and different NUC with additional offset.

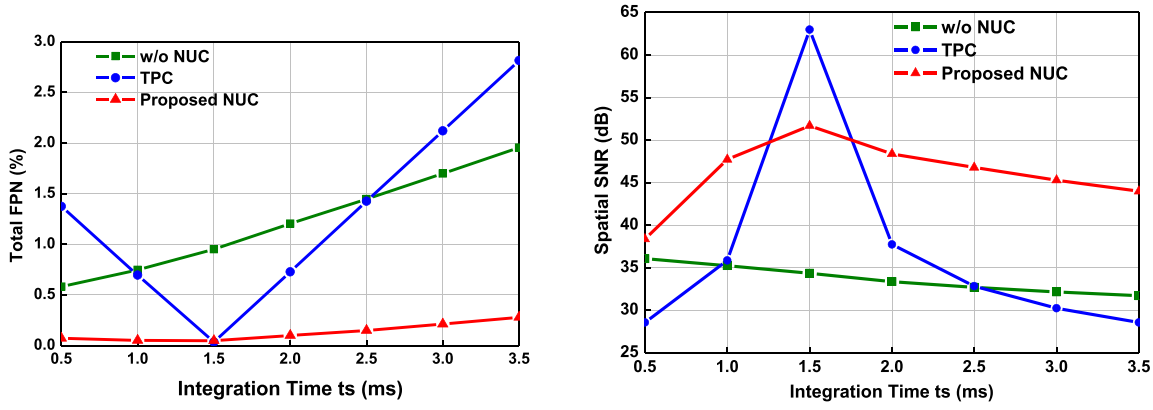

Fig. 5. Measured (a) FPN and (b) spatial SNR of raw image and different NUC with varied integration time t_S.

4.1 Correction for Offset FPN

The correction performance for offset FPN is tested first. Images are captured for uniform target in normal operation, including base image and scene image integrated with 16 μs (t_0) and 1.5 ms ($t_S = t_C$), respectively. Random nonuniform offset is added into both base image and scene image as shown in Fig. 3, and the images with additional offset are corrected by TPC and the proposed method with previously computed correction coefficients.

The measured FPN of image without nonuniformity correction, with TPC and the proposed correction are plotted in Fig. 4, respectively, in which the additional offset FPN is varied from 0 to 1%. When the additional offset FPN is 0, TPC achieves the lowest FPN of 0.4%, while it increases with offset FPN by linear proportion. Thanks to the cancellation by base image, FPN of the proposed correction keeps at 0.05% regardless of the variation of offset. Differing from off-line one-point correction with shutter, the proposed method will not disturb the continuous operation of camera since it performs real-time cancellation in digital domain.

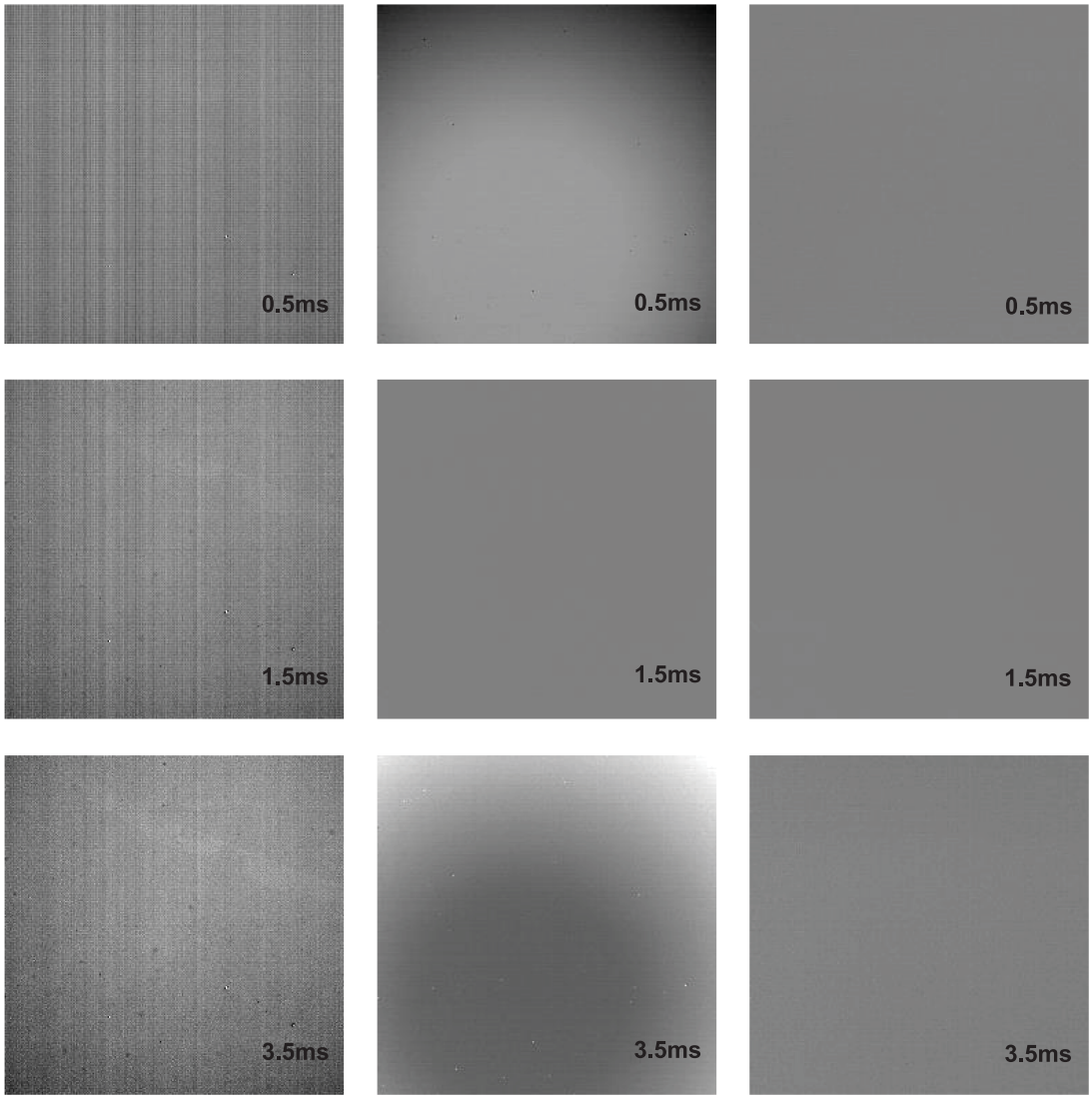

Fig. 6. Sample images for uniform target (a) without NUC, with (b) TPC and (c) the proposed NUC with different integration time t_S.

4.2 Correction for Variable Integration Time

The second experiment evaluates nonouniformity against uniform target for different integration time. Integration time of the base image is fixed as 16 μs (t_0), while scene image is captured with different integration time. The correction coefficients of TPC and the proposed NUC are obtained from off-line calibration with integration time of 1.5 ms (t_C).

The measured FPN of image without NUC, with traditional TPC and the proposed correction are plotted in Fig. 5(a). FPN of raw image rises as increase of integration time since gain FPN is proportional to the integration time. TPC achieves its best performance when the scene image integrated with the same time as in calibration process ($t_S = t_C = 1.5$ ms). However, its FPN deteriorates dramatically if the integration time t_S changes, which increases to 2.8% for $t_S = 3.5$ ms. In contrast, FPN of the proposed method only slightly increases with integration time due to the large attenuation factor in (24), and it is not related with integration time of calibration. As a result, its

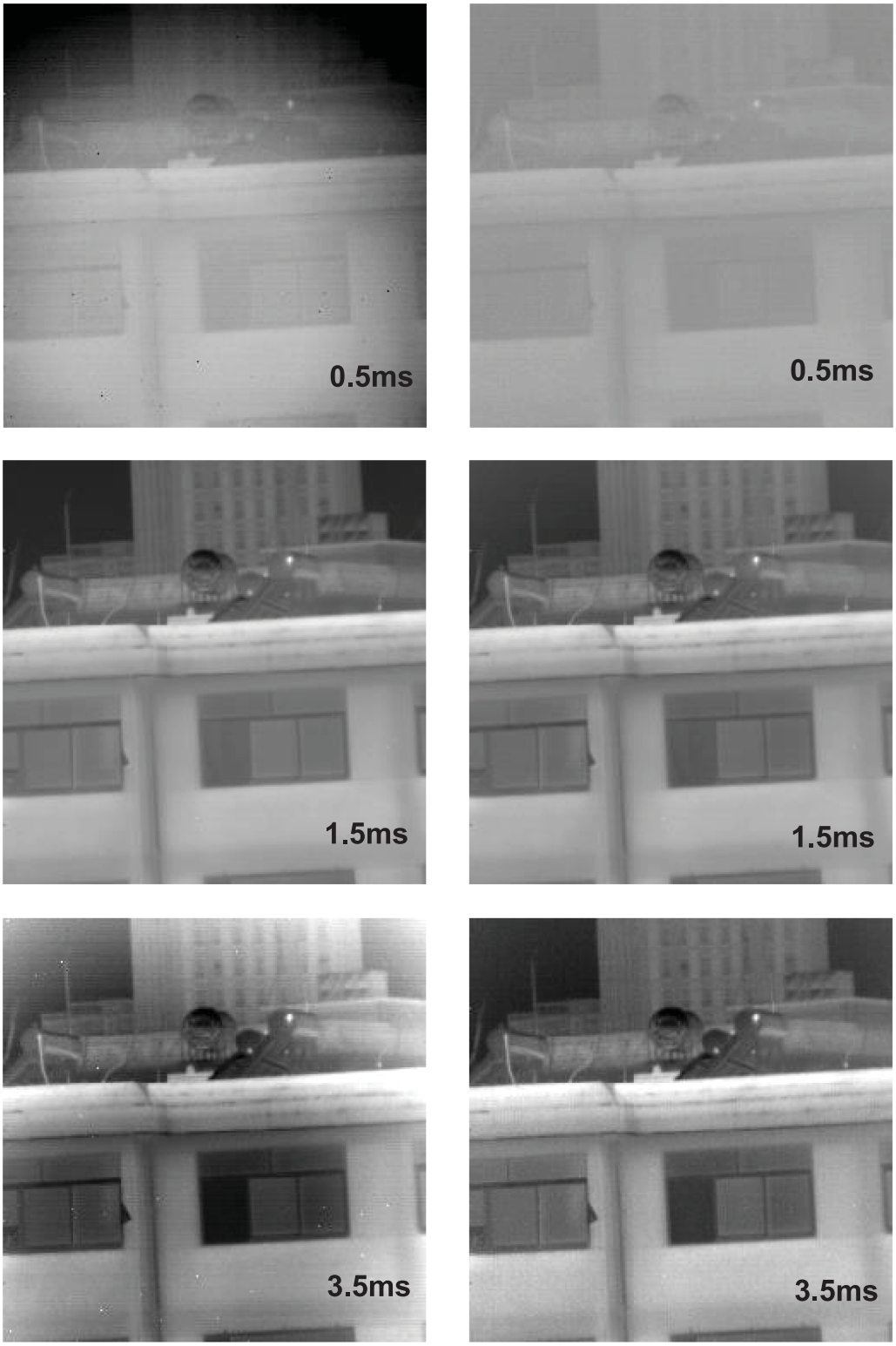

Fig. 7. Sample images for outdoor scene with (a) TPC and (b) the proposed NUC with different integration time t_S.

FPN keeps at a low level (0.05% $\sim$ 0.28%) with same correction coefficients when integration time varies for 7 times (0.5 ms $\sim$ 3.5 ms), which extends the application range with variable integration time.

The spatial SNR is also measured for different schemes shown in Fig. 5(b). PTC exhibits the best SNR when integration time of scene image is same as calibration image as predicted in (12), while when the image integrated with different time, its SNR is degraded severely. The proposal achieves superior SNR versus the variation of integration time. The experimental results confirm the validity of the proposed model and theoretical analysis in previous sections.

Sample images for target with uniform irradiance without NUC, with TPC and the proposed NUC are shown in Fig. 6. When the integration time is same as in calibration process (1.5 ms), both TPC and the proposed NUC achieve good spatial uniformity. Whereas TPC introduces pot-bottom pattern into images when integration time is changed (0.5 ms or 3.5 ms), as well as dark or bright dots and row-to-row stripe noise. Compared to TPC, images after the proposed correction exhibit better uniformity even when integration time changes a lot. The image quality demonstrates good accordance with the measured FPN in Fig. 5.

Thermal images for outdoor scene are also evaluated as shown in Fig. 7. The target at the edge of pot-bottom is corrupted in the image corrected by TPC with 0.5-ms integration, and the dark dots may lead to confusion for the observation of tiny target. The proposed scheme provides better spatial uniformity for the short integration time, even when the image quality is dominated by the temporal random noise due to the low signal power. For long integration time of 3.5 ms, the presented method also exhibits superior performance than TPC.

5. Conclusion

Drawbacks of traditional calibration-based NUC are inspected by the presented analysis model, and a two-dimensional calibration is proposed to deal with the limitation of integration time as well as time-varying offset. In addition to temperature information, different integration time is introduced to calibration process in the proposed method to widen practical application range for variable integration time. Besides, base image with short-time integration is used for real-time cancellation of time-varying offset FPN without additional shutter. Since it only needs to calibrate once, this scheme will not interrupt the normal operation for real scene. The experiments with cooled MWIR camera demonstrate that the presented NUC is effective for various integration times and offset. Compared to scene-based NUC, this method is conducive to practical engineering application because of its low computation complexity and hardware requirement.

References

[1] S. B. Riou, and P. Bermond, "Non uniformity correction and thermal drift compensation of thermal infrared camera," *Proc. SPIE*, vol. 5405, pp. 294–302, 2004.
[2] D. L. Perry and E. L. Dereniak, "Linear theory of nonuniformity correction in infrared staring sensors," *Opt. Eng.*, vol. 32, no. 8, pp. 1854–1859, Aug. 1993.
[3] D. A. Scribner, M. R. Kruer, J. C. Gridley, and K. Sarkady, "Physical limitation to nonuniformity correction in IR focal plane arrays," *Proc. SPIE*, vol. 0865, pp. 185–202, 1988.
[4] A. Friedenberg and I. Goldblatt, "Nonuniformity two-point linear correction errors in infrared focal plane arrays," *Opt. Eng.* vol. 37, no. 4, pp. 1251–1253, Apr. 1998.
[5] A. F. Milton, F. R. Barone, and M. R. Kruer, "Influence of nonuniformity on infrared focal plane arrays performance," *Opt. Eng.*, vol. 24, no. 5. pp. 855–862, Aug. 1985.
[6] M. Schulz and L. Caldwell, "Nonuniformity correction and correctablity of infrared plane arrays," *Infrared Phys. Technol.*, vol. 36, pp. 763–777, Sep. 1995.
[7] R. Wang, P. Chen, and P. Tsien, "An improved nonuniformity correction algorithm for infrared focal plane arrays which is easy to implement," *Infrared Phys. Technol.*, vol. 39, pp. 15–21, Feb. 1998.
[8] Y. Shi, T. Zhang a, Z. Cao, and L. Hui, "A feasible approach for nonuniformity correction in IRFPA with nonlinear response," *Infrared Phys. Technol.*, vol. 46, pp. 329–337, Jul. 2005.
[9] H. X. Zhou, R. Lai, S. Q. Liu, and G. Jiang, "New improved nonuniformity correction for infrared focal plane arrays," *Opt. Commun.*, vol. 245, no. 1, pp. 49–53, Sep. 2005.
[10] H. Yang, Z. Huang, and H. C. Y. Zhang, "Novel real-time nonuniformity correction solution for infrared focal plane arrays based on S-curve model," *Opt. Eng.* vol. 51, no. 7, Jul. 2012, Art. no. 077001.

[11] G. Oh *et al.*, "Implementation of real time non uniformity correction with multiple NUC tables using FPGA in an uncooled imaging system," *Proc. SPIE*, vol. 7298, pp. 2E1–8, 2009.
[12] L. Shkedy, O. Amir, Z. Calahora, J. O. Schelesinger, and I. Szafanek, "Temperature dependence of spatial noise in InSb focal plane arrays," *Proc. SPIE*, vol. 4028, pp. 481–488, 2000.
[13] J. G. Harris and Y. M. Chiang, "Nonuniformity correction of infrared image sequences using the constant-statistics constraint," *IEEE Trans. Image Process.*, vol. 8, no. 8, pp. 1148–1151, Aug. 1999.
[14] Y. Liu, H. Zhu, and Y. Zhao, "Scene-based nonuniformity correction technique for infrared focal-plane arrays," *Appl. Opt.*, vol. 48, no. 12, pp. 2364–2372, Apr. 2009.
[15] E. Vera, P. Meza, and S. Torres, "Total variation approach for adaptive nonuniformity correction in focal-plane arrays," *Opt. Lett.*, vol. 36, no. 2, pp. 172–174, Jan. 2011.
[16] J. Zeng, X. Sui, and H. Gao, "Adaptive image-registration-based nonuniformity correction algorithm with ghost artifacts eliminating for infrared focal plane arrays," *IEEE Photon. J.*, vol. 7, no. 5, Oct. 2015, Art. no. 6308016.
[17] Y. Cao and C. Tisse, "Single-image-based solution for optics temperature-dependent nonuniformity correction in an uncooled long-wave infrared camera," *Opt. Lett.*, vol. 39, no. 6, pp. 646–648, Feb. 2014.
[18] L. Liu and T. Zhang, "Optics temperature-dependent nonuniformity correction via l_0-regularized prior for airborne infrared imaging systems single-image-based solution for optics temperature-dependent nonuniformity correction in an uncooled long-wave infrared camera," *IEEE Photon. J.*, vol. 8, no. 5, Oct. 2016, Art. no. 3900810.
[19] B. Ratliff, M. Hayat, and R. Hardie, "An algebraic algorithm for nonuniformity correction in focal-plane arrays," *J. Opt. Soc. Amer. A*, vol. 19, no. 9, pp. 1737–1747, 2002.